ACS APPLIED MATERIALS & INTERFACES

Research Article

www.acsami.org

Rice-Husk-Templated Hierarchical Porous TiO_2/SiO_2 for Enhanced Bacterial Removal

Dalong Yang,[†,‡] Bin Du,[§,‡] Yaxian Yan,[§] Huiqin Li,[⊥] Di Zhang,[†] and Tongxiang Fan*[,†]

[†]State Key Laboratory of Metal Matrix Composites, [§]School of Agriculture and Biology Department, and [⊥]Instrumental Analysis Center, Shanghai Jiaotong University, Shanghai 200240, People's Republic of China

Supporting Information

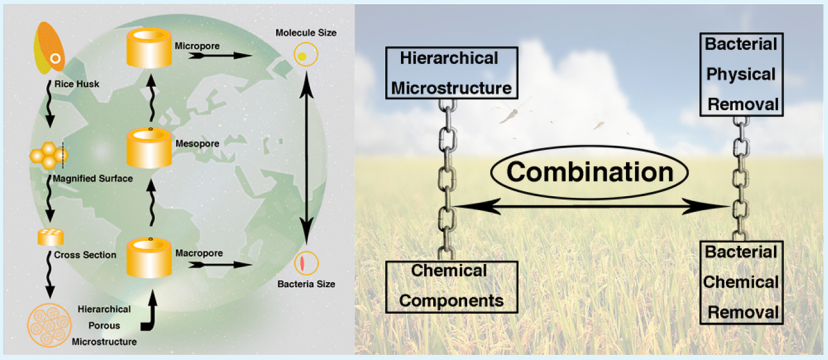

ABSTRACT: To further enhance the bacterial removal capability, we synthesize a biotemplated hierarchical porous material coupling chemical components and hierarchical microstructure, which is derived from rice husk. The results show that the chemical components and hierarchical microstructure of the prepared material could both be factors in enhancing the bacterial removal capability. On the basis of the experimental results, we propose a hypothetical enhanced bacterial removal mechanism model of the prepared material. Furthermore, we propose a hypothetical method of inferring bacterial physical removal effects of samples by their dye adsorption results. Also, the hypothetical method has been proven to be reasonable by the experimental results. This work provides a new paradigm for bacterial removal and can contribute to the development of new functional materials for enhanced bacterial removal in the future.

KEYWORDS: *biotemplate, hierarchical porous material, titanium oxide, silica, bacterial removal*

INTRODUCTION

The current pathogenic bacteria problem remains a great challenge to human society.[1,2] To solve this potential crisis,[3] different methods are applied to the field of bacterial removal; these could be typically classified as either bacterial chemical removal or bacterial physical removal.

Bacterial chemical removal is a process that employs a sterilization effect to destroy bacteria cells, such as ultraviolet (UV) radiation, ozone oxidation, photocatalysis degradation, etc.[4−6] In addition, using functional oxide materials for sterilization has been attracting more and more interest.[7−10] In order to enhance the sterilization effect, the sterilization mechanism is crucial. In the past decades, previous works have proven that the key sterilization mechanisms of oxide materials are the same: the reactive oxygen species are able to easily destroy bacteria, which are produced in the interface between oxides and water.[11−13] However, different oxides have different bacterial removal effects because of their different chemical components. Remarkably, oxide photocatalysts further enhance the UV radiation sterilization effect and possess better sterilization capability than the other oxides without photocatalytic properties under UV irradiation.[11−13] Among the many oxide photocatalysts, titanium dioxide (TiO_2) has been applied to daily life for a long time because of its highly efficient photoactivity, as well as its stability. Unfortunately, however, TiO_2 only adsorbs UV for photoactivity. Consequently, developing an appropriate method of making TiO_2 have highly efficient photoactivity is meaningful, especially within the visible-light range. In this way, the photocatalytic property of TiO_2 could make the sterilization effect under visible-light irradiation possible.

Bacterial physical removal is a process that contains adsorption effects and filtering effects, such as Coulomb force adsorption, microstructure filtering, etc.[14,15] Chemical components of materials could be helpful for the adsorption effect because of the Coulomb force. For example, TiO_2 synthesized by proper methods could have a high isoelectric point, meaning that TiO_2 is positively charged in water, which could be helpful for adsorbing negatively charged bacteria in water, and then the distance between reactive oxygen species and bacterial cells

Received: October 21, 2013
Accepted: February 11, 2014
Published: February 11, 2014

   dx.doi.org/10.1021/am500206g | ACS Appl. Mater. Interfaces 2014, 6, 2377−2385

would be shortened, so that the bacterial removal effect could be further enhanced. Furthermore, the microstructure of materials could be an important factor for bacterial physical removal because of the microstructure adsorption effect. Different kinds of porous materials show advanced functional properties,[16−18] which could be helpful for exploring the microstructure adsorption effect. Compared to most common nanoscale materials,[19−21] materials with hierarchical porous structures display a much better performance in various fields.[22,23] In the field of bacterial removal, the hierarchical porous structure has a high surface area that could be beneficial for producing reactive oxygen species for sterilization, and its adsorption effect could be helpful for bacterial physical removal.[24] Hierarchical porous structures are common in biomass and could be useful for photocatalytic properties.[25] Compared to hierarchical orderly porous material,[16−18] the hierarchical porous materials derived from biomass show two different properties as follows: their pores are disorderly, and they have different scale pores (micropores, mesopores, and macropores) in a wide range.[24,25] The property of different scale pores in a wide range could be suitable for adsorbing bacteria in different sizes because of the microstructure adsorption effect.[24] Thus, the hierarchical porous structure derived from natural biomass could be utilized as a biotemplate to synthesize functional materials for bacterial removal.

A substantial body of previous works have focused on only one aspect of bacterial removal; there are only a few papers reporting methods of combining bacterial chemical removal with bacterial physical removal.[4−10,14,15] Following previous works, we propose rice husk as a biotemplate to synthesize TiO_2 with a precursor containing titanium (Ti) ions. In fact, TiO_2 could be a potentially excellent material for bacterial removal because of its photocatalytic property for an enhanced sterilization effect under a light source and its positively charged property for a high isoelectric point. Because the silicon element is contained in natural rice husk, we expect that it could be converted to silica (SiO_2) by calcinating to synthesize a mixed-oxide system as TiO_2/SiO_2; this could enhance photocatalytic properties for bacterial removal because of the capability of SiO_2 to harvest light within a visible range.[26] In addition, the hierarchical porous property of natural rice husk is expected to be inherited during the synthesis process,[27] resulting in biotemplated hierarchical porous TiO_2/SiO_2, hereafter referred to as BH-TiO_2/SiO_2.

The material prepared here is expected to have a better performance than material without the template because of its potentially enhanced bacterial removal coupling chemical components and hierarchical microstructure. Because *Escherichia coli* is a typical Gram-negative bacterium that is seriously harmful to human health,[28] we chose it as a typical sample for the bacterial removal experiment. Compared with our previous work,[24] the prepared sample of this work effectively took advantage of the chemical component of natural biomass. Furthermore, the differences of the chemical component and microstructure of the prepared material between this work and our previous work could be helpful for exploring new methods to produce advanced bacterial removal materials.[24] In summary, this work provides a new concept for combining bacterial chemical removal with bacterial physical removal. The methodology presented here could be helpful for developing new functional materials with a highly efficient bacterial removal effect in the future.

EXPERIMENTAL SECTION

Synthetic Procedure of the Samples. A titanium trichloride ($TiCl_3$) precursor solution was prepared by dissolving $TiCl_3$ (5% by weight) in a 50% ethanol (EtOH) solution. Natural rice husk was treated with a 5% hydrochloric acid (HCl) solution under vacuum at 10 °C for 24 h to remove potassium (K), calcium (Ca), and sodium (Na) ions, with the color of the rice husk turning from yellow to deep yellow. After being soaked in pure water (H_2O) for 24 h to remove redundant ions, the rice husk was soaked in a $TiCl_3$ precursor solution for 72 h. Because of the existence of many functional groups such as hydroxyls, Ti ions were easily introduced into the rice husk. Afterward, the samples were desiccated in an aerated oven at 25, 60, 80, and 105 °C successively, undergoing each temperature for 2 h. Then, the samples were calcined in air at 1 °C/min to 280 °C for 2 h to remove cellulose of natural rice husk. Finally, the as-treated samples were calcined at 1 °C/min to 500 °C for 2 h for synthesis of the anatase phase. The final products (BH-TiO_2/SiO_2) were obtained after calcination and cooled to room temperature. Common TiO_2 was obtained by calcining the $TiCl_3$ precursor solution directly in the same calcination conditions. Common SiO_2 was synthesized by calcining the mixture solution in the same calcination conditions, and the mixture solution was the solution containing tetraethyl orthosilicate, EtOH, H_2O, and HCl.[29] Natural rice husk was carbonized at 550 °C for 4 h, and then the samples were mixed with a potassium hydroxide (KOH) solution (concentration: 20%). After the mixture had been heated to remove redundant water, it was calcined at 400 °C for 0.5 h of pretreatment and then calcined at 700 °C for 1.5 h of radioactivation. Finally, the product was washed by pure water and then dried to get the activated carbon originating from the rice husk.

Measurement of the *E. coli* Physical Removal Properties of the Samples. Approximately 10^9 colony-forming units per milliliter (CFU/mL) of the *E. coli* strain B were cultured on Luria−Bertani (LB) agar plates. *E. coli* physical removal equipment was designed as follows:[24] one piece of quantitative filter paper of φ = 11 cm and medium speed and one piece of quantitative filter paper of φ = 11 cm and slow speed were folded to form a funnel shape. They were then placed in a Büchner funnel (G3, 60 mL). *E. coli* solutions (10 mL) were filtered with this equipment, and the cell number in the filtrate was then the *E. coli* physical removal effect without any adsorbent. For comparison, 100 mg of different kinds of samples were added in the center of the quantitative filter paper, and 10 mL of *E. coli* solution was filtered with the samples and the *E. coli* physical removal equipment together, so that the *E. coli* number of the filtrate was the *E. coli* physical removal effect of each sample. The aliquot filtrate (1 μL) of each experiment was diluted 10^2, 10^3, and 10^4 in triplicate. After the *E. coli* physical removal experiments, all of the filtrates were cultured on LB agar plates for 18 h at 37 °C. Finally, *E. coli* numbers were determined by counting the colonies on the LB agar plates. All of the experiments were performed under sterile conditions.

Measurement of the *E. coli* Bacteriostatic Properties of the Samples. After being heated at 120 °C for 20 min, 100 mg samples prepared by different methods were placed in a sterile conical flask, to which 50 mL of phosphate-buffered saline (pH = 6.8) was added, followed by 0.5 mL of *E. coli* solution (approximately 10^9 CFU/mL of *E. coli*). After the mixture was mechanically shaken for 24 h at 37 °C, an aliquot (0.1 mL) was diluted 10^2, 10^3, and 10^4 in triplicate, and then the dilutions (0.1 mL) were cultured on LB agar plates for 18 h at 37 °C. The *E. coli* numbers were determined by counting the colonies on the LB agar plates. All of the experiments were performed under sterile conditions.

Measurement of the *E. coli* Chemical Removal Properties of the Samples under a Light Source. To perform the test, five test tubes were placed in a rotary shaker machine at 37 °C under sterile conditions. Each test tube contained 10 mL of *E. coli* solution (approximately 10^8 CFU/mL of *E. coli*) and different kinds of samples (10 mg), except that one test tube contained only *E. coli* solution. A xenon (Xe) lamp (200 W, λ_{main} = 365 nm) was used to apply the light source, and cutoff filters at 400 nm were employed to determine whether to remove wavelengths shorter than 400 nm to obtain the desired visible light. A luxmeter was used to control the irradiation

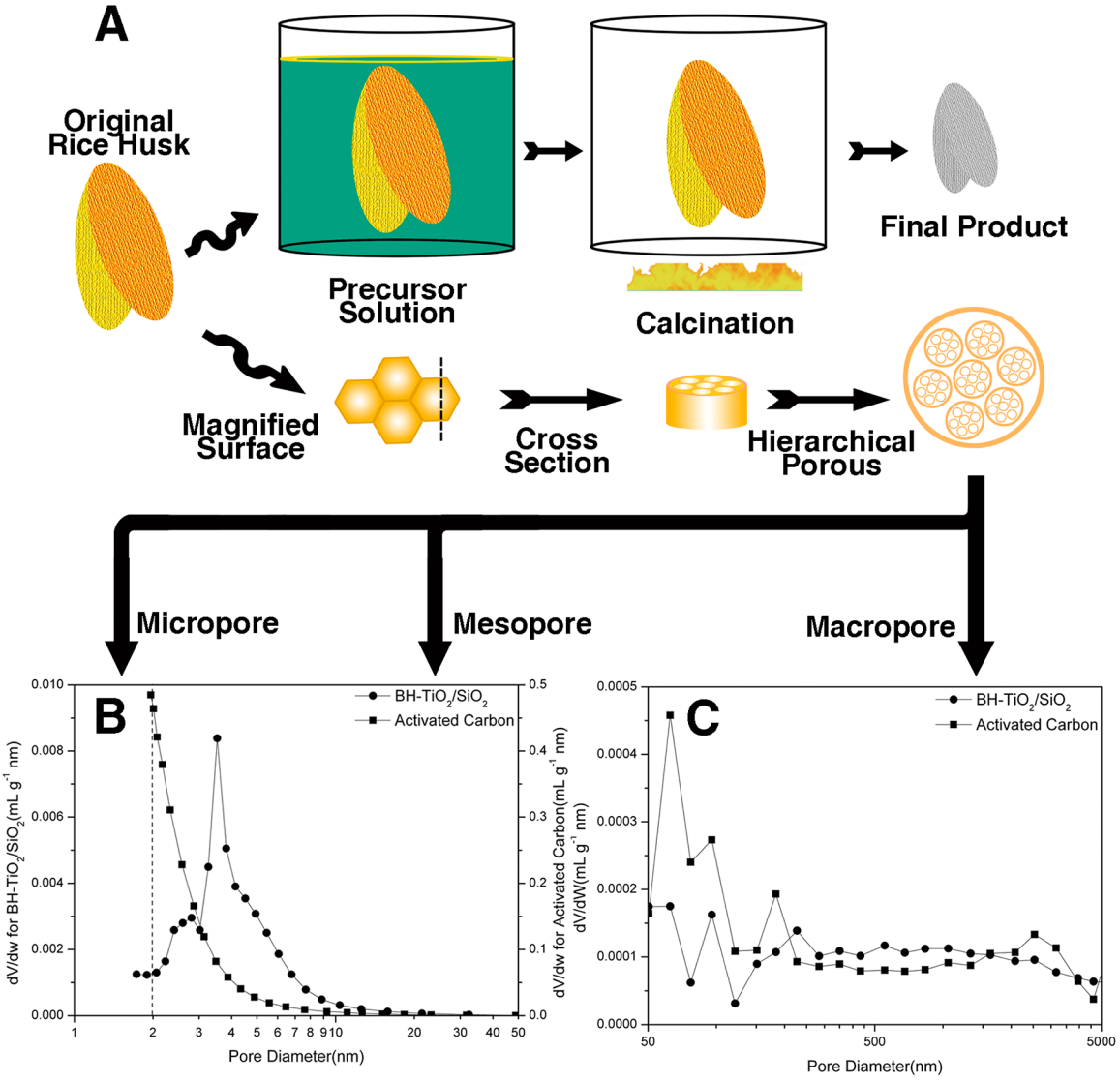

Figure 1. (A) Scheme of the synthetic technology and hierarchical porous structure of the rice husk with gradually magnified images. (B) Micropore-size (less than 2 nm) and mesopore-size (between 2 and 50 nm) distribution curves of the samples originating from the rice husk. (C) Macropore-size (more than 50 nm) distribution curves of the samples originating from the rice husk.

density on the test tubes as 1 mW/cm^2. After 1 h of irradiation, 0.1 mL of solution of each test tube was diluted 10^2, 10^3, and 10^4 in triplicate, and then the dilutions (0.1 mL) were cultured on LB agar plates for 18 h at 37 °C. The *E. coli* numbers were determined by counting the colonies on the LB agar plates. All of the experiments were carried out under sterile conditions.

Characterization of the *E. coli* Sterilization Properties by the Photocatalytic Properties of BH-TiO_2/SiO_2 by Atomic Force Microscopy (AFM) in Situ. The *E. coli* solution (approximately 10^8 CFU/mL of *E. coli*) containing BH-TiO_2/SiO_2 was dropped on the mica sheet for characterization of AFM in situ. A Xe lamp (200 W) was used to apply the UV source, and the irradiation density on the mica sheet was 1 mW/cm^2 controlled by the luxmeter. The irradiation time was 15 min. All of the experiments were carried out under sterile conditions.

Measurement of the Dye Adsorption Effects of the Samples. Adsorption experiments were carried out by agitating the adsorbent (100 mg) with a dye solution (100 mL) at the desired concentration at 180 rpm, 25 °C in a thermostatted rotary shaker. For comparison, four different adsorbents were used: common TiO_2, common SiO_2, BH-TiO_2/SiO_2, and powdered activated carbon originating from the rice husk. Titan yellow ($C_{28}H_{19}N_5Na_2O_6S_4$) and methylene blue ($C_{16}H_{18}ClN_3S$) dyes were used for adsorption as the typical negatively and positively charged dyes. The effects of the adsorbent dosage were studied with 100 mg of adsorbent and 100 mL of 25, 50, 75, and 100 mg/L titan yellow or 2.5, 5, 7.5, and 10 mg/L methylene blue dye solutions at equilibrium time. The adsorption effects were monitored by taking sample solutions at 0, 15, 30, 45, and 60 min during the adsorption process, respectively. Then, these sample solutions were centrifuged with 4000 rpm for 5 min. Finally, the supernatants were tested in sequence using a Perkin-Elmer Lambda 750s UV−vis spectrometer to determine the absorption spectra. Moreover, Freundlich and Langmuir isotherms were employed to study the adsorption capacity of the adsorbent.

RESULTS AND DISCUSSION

Synthesis and Characterization of the Samples. To explore the potential factors for enhanced bacterial removal effects coupling chemical components and hierarchical microstructure, we synthesized BH-TiO_2/SiO_2. For comparison, common TiO_2 that possessed photocatalytic properties for sterilization was used to prove the importance of the hierarchical microstructure for enhanced bacterial removal. Meanwhile, common SiO_2 had a chemical composition similar

dx.doi.org/10.1021/am500206g | ACS Appl. Mater. Interfaces 2014, 6, 2377−2385

to that of BH-TiO_2/SiO_2, which could also be used to prove the importance of the hierarchical microstructure for enhanced bacterial removal. On the other hand, powdered activated carbon originating from the rice husk had microstructure features similar to those of BH-TiO_2/SiO_2, which could be used to prove the importance of the chemical component for enhanced bacterial removal. BH-TiO_2/SiO_2 was a white sample that was synthesized by the simple biotemplate method (Figure 1A), and the size of the product was slightly smaller than the original rice husk.

From field-emission scanning electron microscopy (FESEM), AFM, and transmission electron microscopy (TEM) results (Supporting Information, Figures S1−S3), we could find that BH-TiO_2/SiO_2 was a typical hierarchical porous material that inherited the features of the hierarchical microstructure of the original rice husk; the same was true for the activated carbon originating from the rice husk. The TEM results demonstrated that BH-TiO_2/SiO_2 had amorphous and anatase crystalline phases. The results of the images demonstrated that the hierarchical microstructure of the samples was not destroyed after grinding. The hierarchical three-level micro/meso/macropore-size distribution curves (Figure 1B,C) further demonstrated that the samples originating from the rice husk had a unique hierarchical porous structure. However, there were some differences between BH-TiO_2/SiO_2 and activated carbon originating from the rice husk. The Brunauer−Emmett−Teller (BET) surface results showed that activated carbon originating from the rice husk (1503.8 m^2/g) had a much larger area than BH-TiO_2/SiO_2 (160.2 m^2/g); this could be caused by the difference between their synthesis processes. In addition, activated carbon originating from the rice husk had much greater micropore-size distribution than BH-TiO_2/SiO_2 (Figure 1B), which also confirmed the results of the BET surface area. The nitrogen adsorption results showed that the samples originating from the rice husk were both typical H3-type type IV isotherms. Yet, the porosity results of the samples showed that BH-TiO_2/SiO_2 (83.5%) had a higher porosity than activated carbon originating from the rice husk (68.6%; Supporting Information, Figure S4); this meant that BH-TiO_2/SiO_2 had many more macropores than activated carbon originating from the rice husk (Figure 1C). Especially, both of these samples originating from the rice husk lacked a mesopore-size distribution that was more than 20 nm in diameter (Figure 1B). The microstructure result implied that BH-TiO_2/SiO_2 had a potentially better bacterial physical adsorption and removal function because its macropores were much greater than those of activated carbon originating from the rice husk.

X-ray diffraction (XRD) patterns of different samples showed that common TiO_2 was the typical anatase phase, common SiO_2 was the typical amorphous SiO_2 phase, and activated carbon originating from the rice husk was the typical amorphous carbon phase. However, BH-TiO_2/SiO_2 was the typical anatase phase with the amorphous SiO_2 phase as its background (Supporting Information, Figure S5), which displayed consistency with the TEM results. The crystalline size of BH-TiO_2/SiO_2 was 6.1 nm, and that of common TiO_2 was 15.8 nm. The entire X-ray photoelectron spectroscopy survey of BH-TiO_2/SiO_2 showed the existence of Ti, silicon (Si), oxygen (O), and nitrogen (N).[25] Specially, the phenomenon of N doping could cause BH-TiO_2/SiO_2 to have photocatalytic properties within the visible-light range, which could be utilized for sterilization under visible light in the following bacterial chemical removal experiments.

From ζ-potential results (Supporting Information, Figures S6 and S7), we could prove that common TiO_2 and BH-TiO_2/SiO_2 had a high isoelectric point (around 7); they were nearly neutrally electric in pure water. Yet, common SiO_2 and activated carbon originating from the rice husk had a low isoelectric point (lower than 3), and they were negatively charged in pure water. Simultaneously, methylene blue dye was positively charged in pure water (nearly 9), but titan yellow dye was negatively charged in pure water (lower than 3). Titan yellow was negatively charged in pure water, which was the same as *E. coli*. The ζ-potential results served as a reference for potential Coulomb force adsorption in the following experiments, which could also be utilized for bacterial physical removal. Furthermore, the titan yellow dye adsorption results of the different samples could be a useful reference for *E. coli* physical removal effects; this is because titan yellow dye and *E. coli* were both negatively charged, and the adsorption effects of the prepared materials contained two major adsorption effects: Coulomb force adsorption and microstructure adsorption.[24]

Bacterial Removal of the Samples. The *E. coli* physical removal equipment was applied to compare the different bacterial physical removal efficiencies of the device with and without the four different samples (Supporting Information, Figures S8 and S9).[24] From the *E. coli* physical removal results (Figure 2 and Supporting Information, Table S1), we could

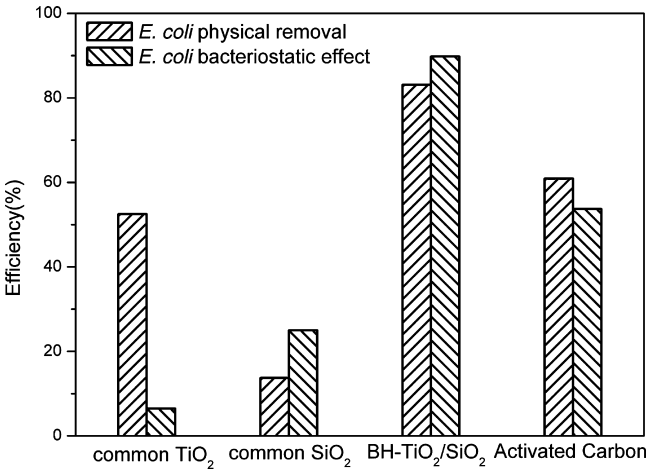

Figure 2. *E. coli* physical removal and *E. coli* bacteriostatic studies.

find that BH-TiO_2/SiO_2 had the best performance because of its two advantages. The first was its higher isoelectric point than activated carbon originating from the rice husk, and the second was its larger surface area and microstructure adsorption effect compared with common TiO_2 and common SiO_2. Moreover, the porosity and pore-size distribution results implied that BH-TiO_2/SiO_2 had much more macropores than activated carbon originating from the rice husk (Figure 1C). In addition, the existence of macropores could be useful for *E. coli* physical adsorption; thus, BH-TiO_2/SiO_2 had a much better performance than activated carbon originating from the rice husk. Furthermore, the results confirmed that the chemical components and hierarchical microstructure were both important points of bacterial physical removal, which could be helpful for the next bacterial removal experiments because of their potentially integrated bacterial removal effects.

The *E. coli* bacteriostatic equipment (Supporting Information, Figure S10) was applied to compare the different bacteriostatic efficiencies of the device with and without the four different samples (Supporting Information, Figures S11 and S12).[30] From the *E. coli* bacteriostatic experiment (Figure 2 and Supporting Information, Table S2), we could find that BH-TiO_2/SiO_2 had the best performance and common TiO_2 had the worst performance. This result showed that the bacteriostatic effect depended on two factors. The first was that the sample could produce sterilization ions for the sterilization effect, which was previously proven by many scientists;[11−13] the second was the microstructure adsorption effect (Supporting Information, Figure S10). The adsorption effect could reduce the distance between the sterilization ions and *E. coli*. Meanwhile, the enrichment of *E. coli* could be helpful for the enhanced sterilization effect. The sterilization effect was mediocre without the adsorption effect of the microstructure, as shown by common TiO_2 and common SiO_2. The result confirmed the advantage of the microstructure adsorption effect, which could be as important as the effect of the sterilization ions.

The *E. coli* chemical removal equipment under a light source (Supporting Information, Figure S13) was designed to compare the different sterilization efficiencies of the device with and without the four different samples under UV or visible-light irradiation (Supporting Information, Figures S14−S17). From the results of the *E. coli* chemical removal properties of the samples (Figure 3 and Supporting Information, Tables S3 and S4), we could find that the number of *E. coli* was reduced under UV irradiation but increased under visible-light irradiation. From the results under UV irradiation, we could find that BH-TiO_2/SiO_2 had the best performance because of its adsorption effect of the microstructure and the large amount of sterilization ions produced by the photocatalytic property of TiO_2 under UV irradiation. Furthermore, common SiO_2 could enhance the light intensity to enhance the sterilization effect of UV, and activated carbon originating from the rice husk could cause the enrichment phenomenon of *E. coli* for the enhanced sterilization effect of UV. Thus, the results under UV irradiation (Figure 3A) showed that all of the sample chemical removal effects were much more obvious than the sterilization effect without samples. Still, the integrated advantages of the chemical components and hierarchical microstructure made BH-TiO_2/SiO_2 have the best performance under UV irradiation, which could also be proven by the results of AFM in situ (Figure 4). All of the cell walls of *E. coli* with BH-TiO_2/SiO_2 were destroyed in 15 min under UV irradiation. From the results under visible-light irradiation (Figure 3B), we could also determine that BH-TiO_2/SiO_2 had the best performance. The rapid growth of *E. coli* was due to visible light; therefore, the sample with the best sterilization effect would have the lowest *E. coli* growth efficiency under visible light. Because visible light favored the growth of *E. coli*, the enrichment of *E. coli* caused by adsorption of the microstructure made activated carbon originating from the rice husk have the most *E. coli* after visible-light irradiation. In addition, common TiO_2 and common SiO_2 showed an invalid chemical removal effect under visible-light irradiation. Specially, BH-TiO_2/SiO_2 had a sterilization effect under visible-light irradiation. The red shifts at the edge of the UV and visible light of BH-TiO_2/SiO_2 and its better photocatalytic property made it produce a sterilization effect under visible-light irradiation.[25] However, *E. coli* grew much faster, but the sterilization ions that were obtained by the photocatalytic property of BH-TiO_2/SiO_2 under visible-light irradiation were not enough; thus, the *E. coli* colony count result of BH-TiO_2/SiO_2 was still more than that of the original *E. coli* solution. The above results showed that the advantage of the hierarchical microstructure was helpful for bacterial chemical removal. Furthermore, the potential mechanism of an enhanced bacterial removal effect could be summarized as follows (Scheme 1): the Coulomb force caused the adsorption effect; the chemical component could be useful in producing more sterilization ions; the adsorption effect of the hierarchical microstructure could reduce the distance between the sterilization ions and *E. coli*, which could also cause the enrichment phenomenon of *E. coli* for the enhanced sterilization effect. Thus, this model could be an advantage to our previous work.[24] Moreover, preparing samples coupling chemical components and hierarchical microstructure was an effective method for enhanced bacterial removal.

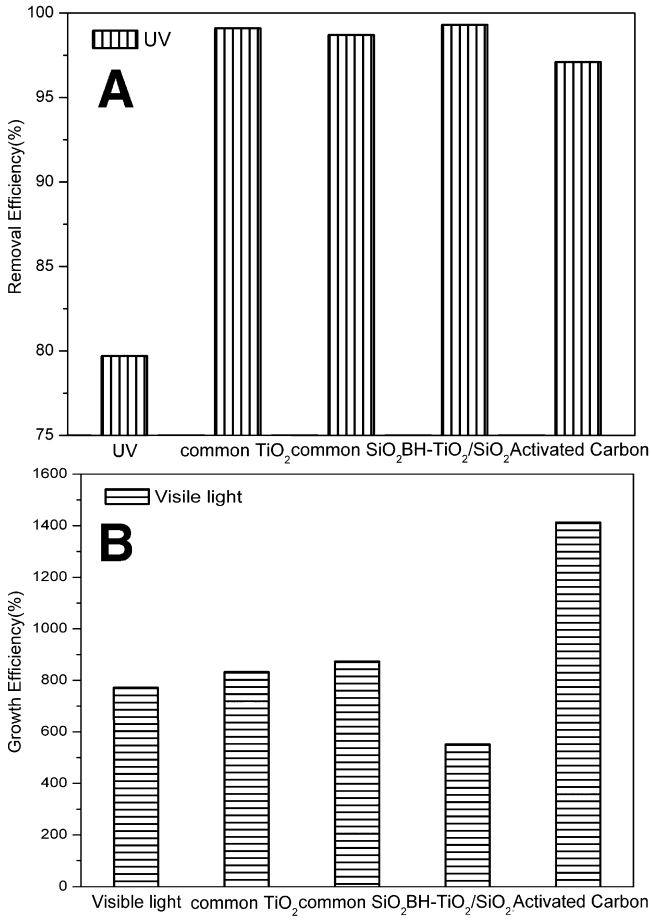

Figure 3. *E. coli* chemical removal studies of different samples under different light sources. (A) Bacterial removal efficiencies under UV irradiation. (B) Bacterial growth efficiencies under visible-light irradiation.

Bacterial Physical Removal Mechanism Research of the Samples. Dye adsorption experiments could serve as a useful reference for bacterial physical adsorption and removal experiments because the size of the dye molecule is suitable for structural adsorption of micro/mesopores; additionally, because the size of the dye molecule is much smaller than that of bacteria, dye adsorption results could reveal the structural adsorption effect of macropores of the prepared material for bacteria. In addition, because bacteria and titan yellow dye are

dx.doi.org/10.1021/am500206g | ACS Appl. Mater. Interfaces 2014, 6, 2377−2385

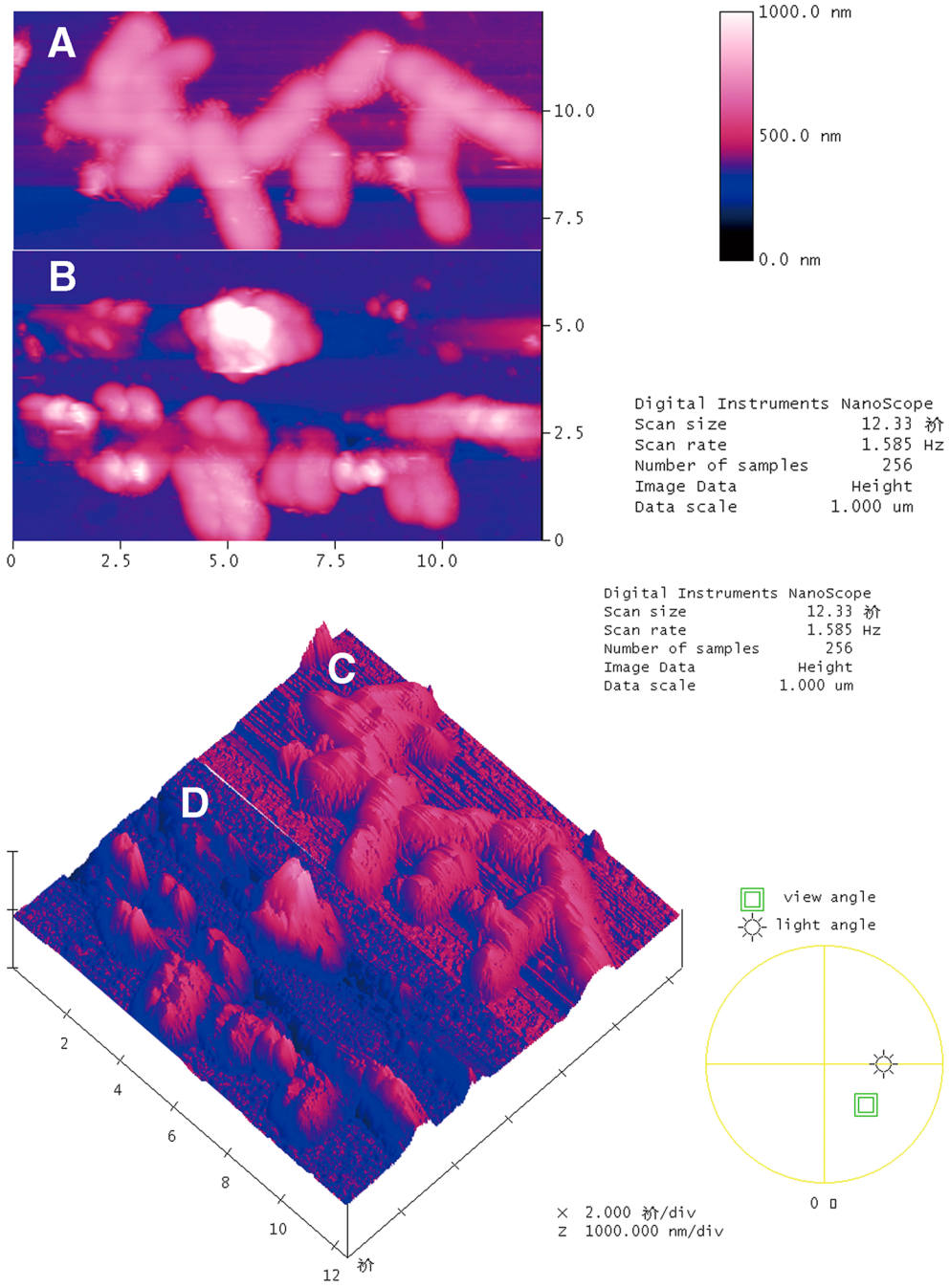

Figure 4. AFM in situ images of *E. coli* with BH-TiO_2/SiO_2 under UV irradiation: (A) before irradiation; (B) after irradiation. AFM in situ 3D images of *E. coli* with BH-TiO_2/SiO_2 under UV irradiation: (C) before irradiation; (D) after irradiation.

both negatively charged in pure water, the adsorption results of titan yellow could be a good reference for the effect of bacterial physical removal. Furthermore, methylene blue dye, which is positively charged in pure water, can produce results that could be a good comparison for exploring the adsorption mechanism of prepared material.

Adsorption kinetic models were applied to interpret the experimental data and determine the mechanism of dye adsorption from aqueous solution.[24] The results showed that all of the adsorbents obeyed the pseudo-second-order equation much better than the pseudo-first-order equation (Figure 5 and Supporting Information, Figures S18−S25). From dye adsorption results, we could find that BH-TiO_2/SiO_2 had the best titan yellow dye adsorption effect but activated carbon originating from the rice husk had the best methylene blue dye adsorption effect; they both had much better adsorption effects than common TiO_2 and common SiO_2. The result implied that the hierarchical porous microstructure of the samples played an important role in the dye adsorption process, as well as the electrical properties of the samples. At first, BH-TiO_2/SiO_2 was neutrally electric in pure water and titan yellow dye was negatively charged in pure water. Although activated carbon originating from the rice husk that was also negatively charged had many more micropores and a larger surface area than BH-TiO_2/SiO_2, the adsorption rate of titan yellow dye of the former was obviously slower than the latter. Moreover, activated carbon originating from the rice husk had a much faster methylene blue adsorption rate than BH-TiO_2/SiO_2

Scheme 1. Hypothetical Enhanced Bacterial Removal Mechanism Model

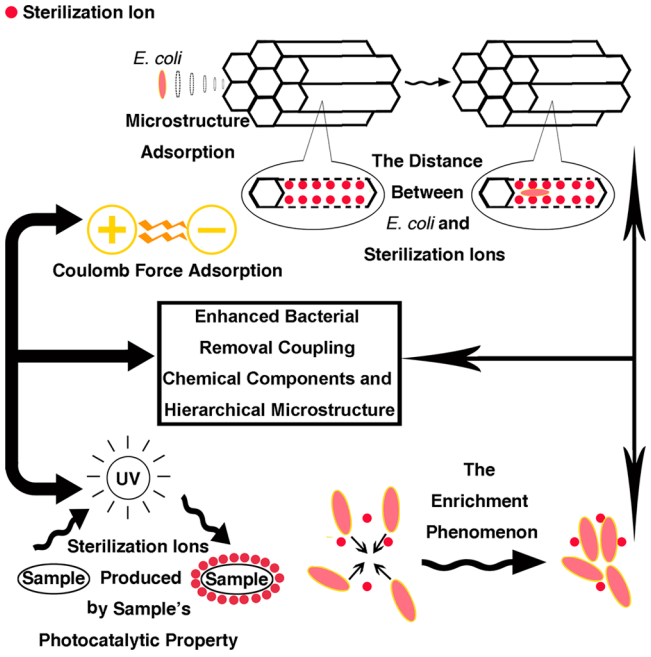

because of the positively charged property of methylene blue. The results demonstrated the importance of the hierarchical porous microstructure and electrical property caused by the chemical components. On the one hand, the porous structure in nanoscale provided a higher surface area for dye adsorption, the micro/mesoporous structure had a suitable size for dye molecule adsorption, and the macroporous structure was helpful for the transmission of dye molecules. On the other hand, the Coulomb force could be a useful factor for the dye adsorption process.

However, we could not find the multimolecular layer adsorption phenomenon among the adsorption results that were all monomolecular layer adsorption (Table 1 and Supporting Information, Figures S26 and S27). Compared to the sample originating from other biomasses of our previous work,[24] the samples originating from the rice husk of this work lacked some mesopores whose pore-size distribution was between 20 and 50 nm in diameter (Figure 1B). This was the key factor for the multimolecular layer adsorption phenomenon. For the multimolecular layer adsorption effect of dye molecules, there should be many suitable pores for microstructure adsorption a second time (Scheme 2A–C), after the preceding Coloumb force adsorption.[24] Therefore, the ideal material for multimolecular layer adsorption should have a pore-size distribution in a wide range; this, however, was

Table 1. Adsorption Isotherms for Different Samples and Dyes

dye/sample	TiO_2	SiO_2	BH-TiO_2/SiO_2	AC[c]
TY[a]	Langmuir	Freundlich	Freundlich	Freundlich
MB[b]	Langmuir	Langmuir	Langmuir	Langmuir

[a]Titan yellow. [b]Methylene blue. [c]Activated carbon.

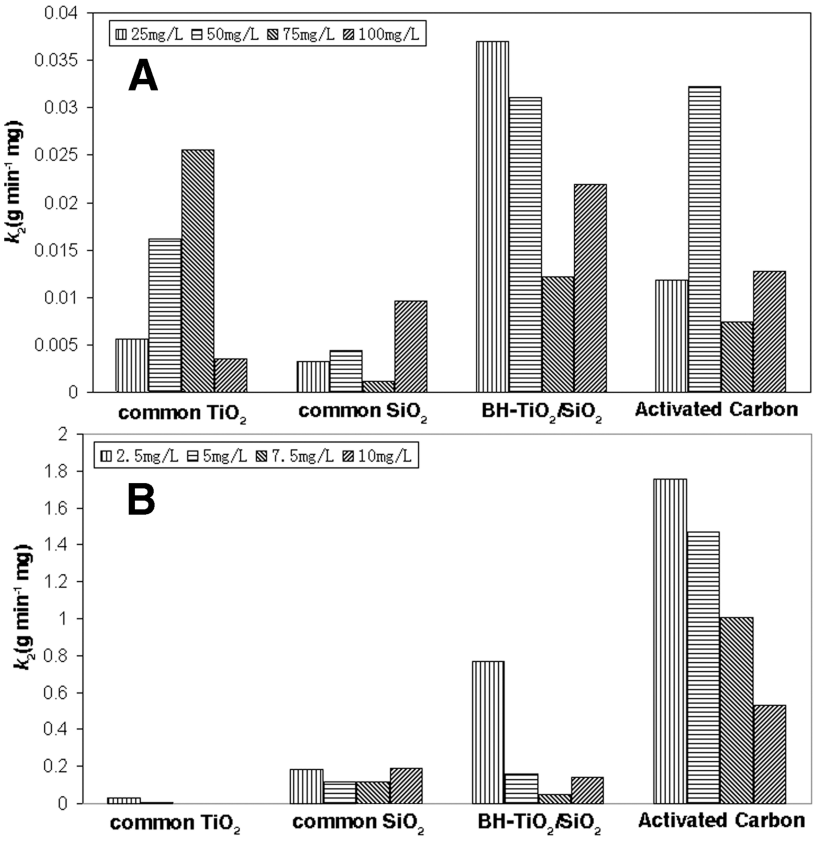

Figure 5. Pseudo-second-order kinetic studies for different adsorbents and dye solutions with different concentrations: (A) titan yellow; (B) methylene blue.

dx.doi.org/10.1021/am500206g | ACS Appl. Mater. Interfaces 2014, 6, 2377–2385

Scheme 2. Dye Adsorption Mechanism Model and Bacterial Physical Removal Mechanism Model: (A) Coloumb Force Adsorption; (B) Microstructure Adsorption; (C) Key Point for Multimolecular Layer Adsorption; (D) Hypothetical Method To Infer Bacterial Physical Removal Capability from the Dye Adsorption Effect

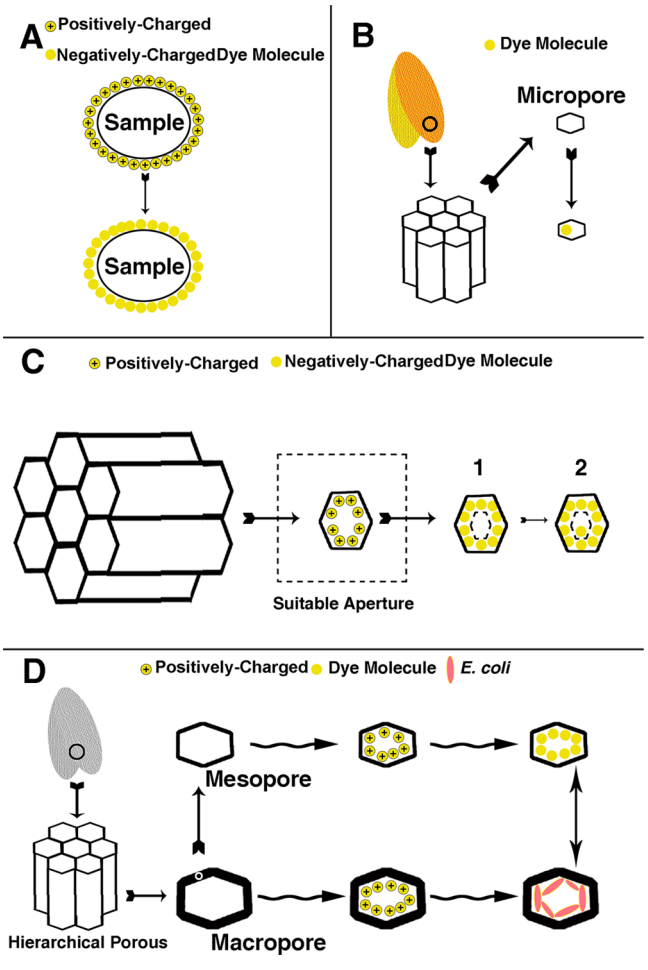

different from our samples originating from the rice husk in which they both lacked mesopore-size distribution with more than a 20 nm diameter. Thus, these results could be a good supplement to our hypothetical model of previous work.[24] The dye adsorption results implied that BH-TiO_2/SiO_2 could be a suitable material for bacterial physical adsorption and removal because of its larger surface area and microstructure adsorption effect compared with common TiO_2 and common SiO_2. Conversely, bacteria were negatively charged in water, and BH-TiO_2/SiO_2 had a higher isoelectric point than activated carbon originating from the rice husk, so the Coulomb force adsorption could be helpful for BH-TiO_2/SiO_2 to enhance the bacterial physical adsorption and removal effect compared with activated carbon originating from the rice husk. The advantages of BH-TiO_2/SiO_2 coupling chemical components and hierarchical porous microstructure could be the potentially helpful elements for enhancing the bacterial removal effect in the bacterial removal experiments.

Furthermore, we found that the bacterial physical removal effects of the samples could be inferred by their dye adsorption results, based on the experimental results (Figures 2 and 5). So, we proposed a hypothetical method (Scheme 2D), and this hypothetical method may be a useful reference for bacterial removal study in the future. Because dye adsorption experiments were low-risk and low-cost compared to bacterial removal experiments, we could perform dye adsorption experiments to test the capabilities of the samples instead of using bacterial physical removal experiments. Also, this method could make the production process much more concise. Moreover, this method could be an advantage to our previous work.[24]

CONCLUSIONS

This work provides a new concept for combining the chemical components with hierarchical porous microstructure to further enhance a bacterial removal effect of the material. The results show that the prepared material coupling chemical components and hierarchical microstructure has a much better performance than other materials in bacterial removal experiments. So, we propose an enhanced bacterial removal mechanism model. Furthermore, we have carried out dye adsorption experiments to infer the bacterial physical removal performance of the samples, and this hypothetical method has been proven to be reasonable by the bacterial physical removal results of the samples. Moreover, this hypothetical method could be applied to the field of bacterial removal and make the production process much more concise. This work could be helpful for developing new functional materials with highly efficient bacterial removal effects in the future.

ASSOCIATED CONTENT

Supporting Information

Experimental section, FESEM, AFM, and TEM images, adsorption−desorption isotherms, XRD patterns, ζ potentials, *E. coli* removal effect images, *E. coli* bacteriostatic and chemical removal under light-source equipment images, pseudo-first-order and pseudo-second-order studies, adsorption isotherm studies, and tables of *E. coli* colony count. This material is available free of charge via the Internet at http://pubs.acs.org.

AUTHOR INFORMATION

Corresponding Author

*Tel.: +86-21-54747779. Fax: +86-21-34202749. E-mail: txfan@sjtu.edu.cn.

Author Contributions

‡Authors who contributed equally.

Notes

The authors declare no competing financial interest.

ACKNOWLEDGMENTS

The authors are grateful for financial support from the National Natural Science Foundation of China (Grant 50972090) and the Research Fund for the Doctoral Program of Higher Education (Grant 20100073110065).

REFERENCES

(1) Mi, Y.; Liu, X.; Zhao, J.; Ding, J.; Feng, S. S. Multimodality treatment of Cancer with Herceptin Conjugated, Thermomagnetic Iron Oxides and Docetaxel Loaded Nanoparticles of Biodegradable Polymers. *Biomaterials* **2012**, *33*, 7519−7529.

(2) Wetzel, S.; Bon, R. S.; Kumar, K.; Waldmann, H. Biology-Oriented Synthesis. *Angew. Chem., Int. Ed.* **2011**, *50*, 10800−10826.

(3) Noah, E. M.; Chen, J.; Jiao, X.; Heschel, I.; Pallua, N. Impact of Sterilization on The Porous Design and Cell Behavior in Collagen Sponges Prepared for Tissue Engineering. *Biomaterials* **2002**, *23*, 2855−2861.

(4) Sato, T.; Miyahara, T.; Doi, A.; Ochiai, S.; Urayama, T.; Nakatani, T. Sterilization Mechanism for Escherichia coli by Plasma Flow at Atmospheric Pressure. *Appl. Phys. Lett.* **2006**, *89*, 073902.
(5) Eto, H.; Ono, Y.; Ogino, A.; Nagatsu, M. Low-Temperature Sterilization of Wrapped Materials Using Flexible Sheet-Type Dielectric Barrier Discharge. *Appl. Phys. Lett.* **2008**, *93*, 221502.
(6) Liou, J. W.; Chang, H. H. Bactericidal Effects and Mechanisms of Visible Light-Responsive Titanium Dioxide Photocatalysts on Pathogenic Bacteria. *Arch. Immunol. Ther. Exp.* **2012**, *60*, 267−275.
(7) Nie, Z.; Kumacheva, E. Patterning Surfaces with Functional Polymers. *Nat. Mater.* **2008**, *7*, 277−290.
(8) Limb, A. J.; Bikondoa, O.; Muryn, C. A.; Thornton, G. Visualization of Complex-Anion Site Conversion on a Metal Oxide Surface. *Angew. Chem., Int. Ed.* **2007**, *46*, 549−552.
(9) Cao, B.; Xu, H.; Mao, C. Controlled Self-Assembly of Rodlike Bacterial Pili Particles into Ordered Lattices. *Angew. Chem., Int. Ed.* **2011**, *50*, 6264−6268.
(10) Li, D.; Mathew, B.; Mao, C. Biotemplated Synthesis of Hollow Double-Layered Core/Shell Titania/Silica Nanotubes under Ambient Conditions. *Small* **2012**, *8*, 3691−3697.
(11) Lipovsky, A.; Tzitrinovich, Z.; Friedmann, H.; Applerot, G.; Gedanken, A.; Lubart, R. EPR Study of Visible Light-Induced ROS Generation by Nanoparticles of ZnO. *J. Phys. Chem. C* **2009**, *113*, 15997−16001.
(12) Karlsson, H.; Cronholm, P.; Gustafsson, J.; Moller, L. Copper Oxide Nanoparticles are Highly Toxic: a Comparison between Metal Oxide Nanoparticles and Carbon Nanotubes. *Chem. Res. Toxicol.* **2008**, *21*, 1726−1732.
(13) Hu, C.; Hu, X.; Guo, J.; Qu, J. Efficient Destruction of Pathogenic Bacteria with NiO/$SrBi_2O_4$ under Visible Light Irradiation. *Environ. Sci. Technol.* **2006**, *40*, 5508−5513.
(14) Wegmann, M.; Michen, B.; Luxbacher, T.; Fritsch, J.; Graule, T. Modification of Ceramic Microfilters with Colloidal Zirconia to Promote the Adsorption of Viruses from Water. *Water Res.* **2008**, *42*, 1726−1734.
(15) Carter, M. J. Enterically Infecting Viruses: Pathogenicity, Transmission and Significance for Food and Waterborne Infection. *J. Appl. Microbiol.* **2005**, *98*, 1354−1380.
(16) Ariga, K.; Vinu, A.; Yamauchi, Y.; Ji, Q.; Hill, J. P. Nanoarchitectonics for Mesoporous Materials. *Bull. Chem. Soc. Jpn.* **2012**, *85*, 1−32.
(17) Li, J. R.; Sculley, J.; Zhou, H. C. Metal−Organic Frameworks for Separations. *Chem. Rev.* **2012**, *112*, 869−932.
(18) Parlett, C. M. A.; Wilson, K.; Lee, A. F. Hierarchical Porous Materials: Catalytic Applications. *Chem. Soc. Rev.* **2013**, *42*, 3876−3893.
(19) Yang, D.; Chen, S.; Huang, P.; Wang, X.; Jiang, W.; Pandoli, O.; Cui, D. Bacteria-Template Synthesized Silver Microspheres with Hollow and Porous Structures as Excellent SERS Substrate. *Green Chem.* **2010**, *12*, 2038−2042.
(20) Hu, C.; Yang, D.; Wang, Z.; Yu, L.; Zhang, J.; Jia, N. Improved EIS Performance of an Electrochemical Cytosensor Using Three-Dimensional Architecture Au@BSA As Sensing Layer. *Anal. Chem.* **2013**, *85*, 5200−5206.
(21) Wang, X.; Yang, D. P.; Huang, P.; Li, M.; Li, C.; Chen, D.; Cui, D. Hierarchically Assembled Au Microspheres and Sea Urchin-Like Architectures: Formation Mechanism and SERS Study. *Nanoscale* **2012**, *4*, 7766−7772.
(22) Chen, L. H.; Li, X. Y.; Tian, G.; Li, Y.; Rooke, J. C.; Zhu, G. S.; Qiu, S. L.; Yang, X. Y.; Su, B. L. Highly Stable and Reusable Multimodal Zeolite TS-1 Based Catalysts with Hierarchically Interconnected Three-Level Micro-Meso-Macroporous Structure. *Angew. Chem., Int. Ed.* **2011**, *50*, 11156−11161.
(23) Schnepp, Z.; Yang, W.; Antonietti, M.; Giordano, C. Biotemplating of Metal Carbide Microstructures: The Magnetic Leaf. *Angew. Chem., Int. Ed.* **2010**, *49*, 6564−6566.
(24) Yang, D.; Fan, T.; Zhang, D.; Zhu, J.; Wang, Y.; Du, B.; Yan, Y. Biotemplated Hierarchical Porous Material: The Positively Charged Leaf. *Chem.—Eur. J.* **2013**, *19*, 4742−4747.
(25) Yang, D.; Fan, T.; Zhou, H.; Ding, J.; Zhang, D. Biogenic Hierarchical TiO_2/SiO_2 Derived from Rice Husk and Enhanced Photocatalytic Properties for Dye Degradation. *PLOS One* **2011**, *6*, e24788.
(26) Anderson, C.; Bard, A. J. Improved Photocatalytic Activity and Characterization of Mixed TiO_2/SiO_2 and TiO_2/Al_2O_3 Materials. *J. Phys. Chem. B* **1997**, *101*, 2611−2616.
(27) Wang, Y.; Feng, C.; Jin, Z.; Zhang, J.; Yang, J.; Zhang, S. A Novel N-doped TiO_2 with High Visible Light Photocatalytic Activity. *J. Mol. Catal. A: Chem.* **2006**, *260*, 1−3.
(28) Mellmann, A.; Harmsen, D.; Cummings, C. A.; Zentz, E. B.; Leopold, S. R.; Rico, A.; Prior, K.; Szczepanowski, R.; Ji, Y.; Zhang, W.; McLaughlin, S. F.; Henkhaus, J. K.; Leopold, B.; Bielaszewska, M.; Prager, R.; Brzoska, P. M.; Moore, R. L.; Guenther, S.; Rothberg, J. M.; Karch, H. Prospective Genomic Characterization of the German Enterohemorrhagic Escherichia coli O104:H4 Outbreak by Rapid Next Generation Sequencing Technology. *PLOS One* **2011**, *6*, e22751.
(29) Panels, J. E.; Joo, Y. L. Incorporation of Vanadium Oxide in Silica Nanofiber Mats via Electrospinning and Sol−Gel Synthesis. *J. Nanomater.* **2006**, *2006*, 1−10.
(30) Huang, L.; Li, D. Q.; Lin, Y. J.; Wei, M.; Evans, D. G.; Duan, X. Controllable Preparation of Nano-MgO and Investigation of Its Bactericidal Properties. *J. Inorg. Biochem.* **2005**, *99*, 986−993.